JMEPEG (2012) 21:2067–2073
DOI: 10.1007/s11665-012-0132-4

1059-9495/$19.00

Contact Reactive Joining of TA15 and 304 Stainless Steel Via a Copper Interlayer Heated by Electron Beam with a Beam Deflection

Binggang Zhang, Ting Wang, Guoqing Chen, and Jicai Feng

(Submitted September 27, 2010; in revised form July 1, 2011)

TA15 titanium alloy and 304 stainless steel were joined via a copper interlayer heated by electron beam with a beam deflection towards the stainless steel. Microstructures of the joints were analyzed by optical microscopy, scanning electron microscopy, and X-ray diffraction. The tensile strengths of the joints and the ultramicrohardness of the intermetallic compounds were also measured. The results showed that the joint was formed by three kinds of metallurgical processes. Copper interlayer and TA15 were joined by contact reaction with the reaction products of CuTi, Cu_4Ti_3, and Cu_2Ti. While copper interlayer and 304 stainless steel were joined by fusion and solid state diffusion process. Tensile strength of the joint can reach to 300 MPa, equivalent to 55% of that of 304 stainless steel. Furthermore, the tensile strength was mostly dependent on the volume of the unmelted copper sheet, although the intermetallics layer was the weakest location in the joint.

Keywords beam deflection, electron beam, microstructure, 304 stainless steel, TA15 titanium alloy, ultramicrohardness

1. Introduction

Recently, composite structures of dissimilar metals were gradually appreciated in national defense and civil industrial fields, such as aeronautics and astronautics, energy, and electric power industries. Combination of the titanium alloy and stainless steel can make full use of the advantages of these two materials simultaneously. Partly replacing stainless steel by the titanium alloy in the components will become an important way to reduce the weight of the spacecrafts (Ref 1, 2).

Fusion welding is infeasible to join titanium alloy and stainless steel owing to their metallurgical incompatibility. Hence solid state joining is one of the viable solutions to overcome this difficulty (Ref 3). However, direct joining was also very difficult due to the low solubility of iron in alpha titanium at room temperature. Qin et al. (Ref 4) have shown that when titanium was directly diffusion bonded to stainless steel, intermetallics like σ-phase, Fe_2Ti and FeTi were produced in the interface by interdiffusion among elements in the base metals which resulted in embrittlement of the joints (both the strength and the ductility of the joint were lowered significantly). Orhan et al. (Ref 5) have suggested that formation of Fe-Cr-Ti intermetallics would even compromise the mechanical properties more indignantly. On the other hand, Aleman et al. (Ref 6) reported that the other factor for the crack formation. A large internal stress was formed due to the difference of linear expansion and thermal conductivity between titanium and iron. Currently, the indirect joining is mostly realized by adding an intermediate metal layer such as nickel, silver, aluminum, and copper foils which can prevent the atomic diffusion between Ti and Fe, Cr or Ni (Ref 7-10). Among these interlayer metals, copper is considered as the best candidate. Copper does not produce brittle intermetallics when joined with iron, chromium, nickel, and carbon. So copper alloy and stainless steel can be directly welded easily by diffusion joining and fusion welding (Ref 11, 12). Moreover, it is a soft metal which weakens and accommodates the stress caused by the mismatch of linear expansion coefficient. It also has a relatively low price compared to other soft metals such as Ag, Au, or Pt.

In the above literatures, copper was used as an interlayer in the diffusion bonding process. The whole metallic materials of the specimens were heated to the elevated temperature, which is not permitted in some occasions. In addition, the diffusion process needs a long time to implement in general. Therefore, some researchers tried to utilize the Ti-Cu contact reaction in the joining process to shorten the time. Wu et al. (Ref 13) have investigated the formational process of liquid in interface of Ti/Cu in detail and proved that the contact reaction can occur in a short time. Uzunov et al. (Ref 14) obtained a highly qualified joint of titanium alloy by contact reaction between titanium and copper via a copper layer. Based on the previous work, a new process for joining titanium alloy and stainless steel was proposed in this paper. A "hybrid joint" between titanium alloy and stainless steel was obtained using a copper interlayer heated by electron beam which can supply high energy instantaneously. In this way, only a small heat-affected zone can be produced and the process can be finished in a shorter period. The "hybrid joint" means that the contact reaction between titanium and copper, fusion welding and solid state

Binggang Zhang, Ting Wang, Guoqing Chen, and **Jicai Feng**, State Key Laboratory of Advanced Welding and Joining, Harbin Institute of Technology, Harbin 150001, People's Republic of China. Contact e-mails: Chenguoqing@hit.edu.cn and fgwangting@163.com.

diffusion bonding devote to the joining process simultaneously in a short time via a beam deflection towards the stainless steel plate. However, this kind of joint structure was hardly reported before. In this paper, the three kinds of metallurgical processes were studied in detail and the mechanical properties were also tested to summarize the new process.

2. Experimental

Materials applied in this experiment were near α-type titanium alloy TA15 and 304 austenitic stainless steel. Their chemical compositions, physical properties are given in Tables 1, 2, and 3. Table 3 illustrates that there are great differences in thermal conductivity and linear expansion coefficient between the two base metals which would lead to large temperature gradient and thermal stress in the joint during welding process. The metals were machined into 50 mm × 25 mm × 2.5 mm plates, and then mechanically and chemically cleaned before welding. 0.5-mm-thick copper sheets were adopted as transition layers and placed in the contact faces. A constant force of 1000 N was applied to the specimens in the direction perpendicular to the contact face by using calibrated springs fixed on the jig. The fixing schematic diagram is shown in Fig. 1.

In order to avoid the fusion of titanium alloy during welding process, the electron beam was acted on the stainless steel plate 0.2 mm away from the interface between copper interlayer and the stainless steel. The welding parameters were experientially selected. The accelerating voltage (U) and focusing current (I_f) were fixed at 55 kV and 2450 mA. Two sets of the welding speed (v) of 5×10^{-3} and 8.33×10^{-3} m s^{-1} and beam current (I_b) of 11 and 13 mA were used to investigate the influence of heat input on the microstructures and the tensile strengths of the joints. Post-heating treatment was conducted by a defocused electron beam repeated four times with a travel speed of 8.33×10^{-3} m s^{-1} and the beam currents of 6, 4, 2, and 2 mA, respectively, in order to reduce the residual stress caused by the heat mismatch between the two base metals.

Specimens for metallographical analysis were wire cut perpendicular to welding directions from the welded joints, then polished and etched. Microstructural examination was implemented on an optical microscope and a S4700 type scanning electronic microscope. X-ray diffraction (XRD) analysis of the fracture surface of the joint after tensile test was carried out on a D/max-rb gyrating anode XRD analysis meter. The operating voltage was 50 kV and the current was 25 mA using a Cu target. Scanning span was 20°-100° (2θ) with a speed of 3° per minute. The phase was identified according to the standard PDF card and Jade software. The mechanical property of the joint was evaluated according to ultramicrohardness (UMH) measured on a DUH-W201 type UMH tester under test force of 100 mN and tensile strength was tested on a Instron 5500R type universal testing machine. The tensile samples were prepared according to ASTM E8M-04 (Ref 15). The tension orientation was perpendicular to the interfaces and the displacement speed was 8.33 μm s^{-1}.

Table 1 Chemical composition of TA15 titanium alloy

Al	Zr	Mo	V	Ti
5.5-7.0	1.5-2.5	0.5-2.0	0.8-2.5	Bal

Table 2 Chemical composition of 304 stainless steel

C	Ni	Cr	Mn	Si	Fe
≤0.07	8-11	17-19	≤2.0	≤1.0	Bal

Table 3 Physical properties of TA15 titanium alloy and 304 stainless steel

Alloy type	Melting point, °C	Specific heat, J kg^{-1} K^{-1}	Thermal conductivity, W m^{-1} K^{-1}	Linear expansion coefficient, 10^{-6} K^{-1}
TA15	1677	539	13.8	8.2
304	1450	502	14.6	16.0

3. Results and Discussion

3.1 Macrostructure of the Cross Section

The macrostructure of the cross section of the joint is given in Fig. 2. It is clear that the welding pool was formed between the copper sheet and the stainless steel by the beam deflection. As a result, mixing of Ti and Fe, Ni or Cr was avoided, and brittle compounds of Ti and Fe, Cr or Ni can not be produced. Metallurgical joining was realized through three kinds of

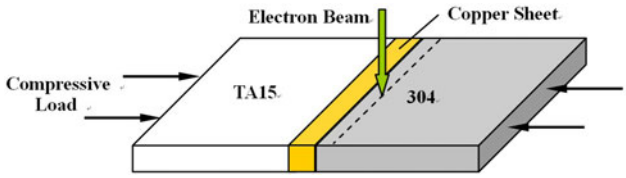

Fig. 1 Schematic diagram of the welding process

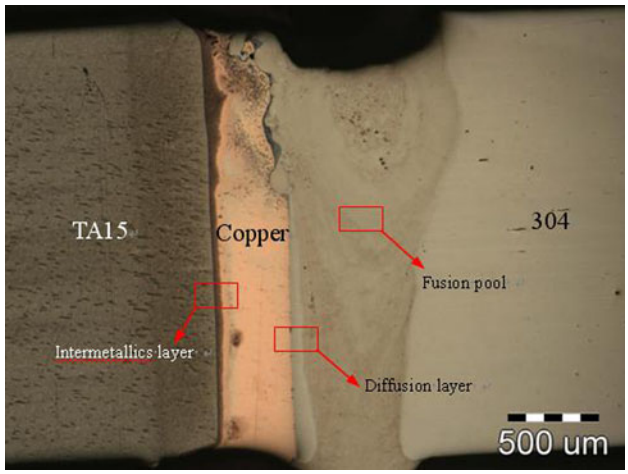

Fig. 2 Macrostructure of cross section of joint

metallurgical processes in the joint. TA 15 and copper sheet were joined by the contact reaction of Ti and Cu. The joining of copper sheet and stainless steel was completed by two different ways—fusion welding at the top of the joint and diffusion bonding at the bottom of the joint. Each process was discussed in detail by observing the high magnification microstructures in the locations marked in Fig. 2.

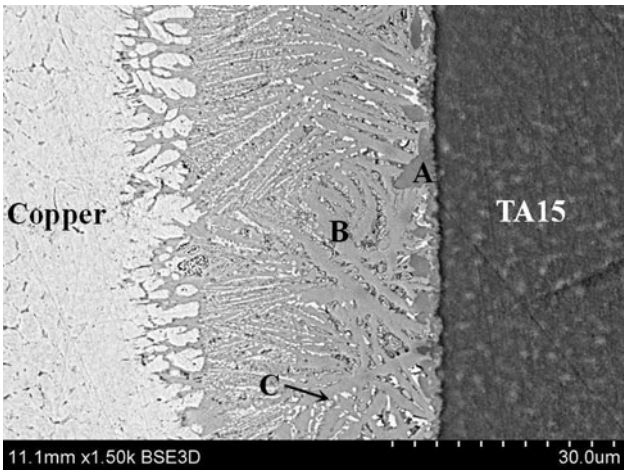

Fig. 3 Microstructure of reaction layer between TA15 and copper sheet

Table 4 Compositions of main elements in various phases (at.%)

	Al	Ti	Cu
A	3	47	48
B	3	40	55
C	2	33	64

3.2 Analysis of the Three Kinds of Metallurgical Process

3.2.1 Contact Reaction of Cu and Ti. The microstructure of the reaction layer between TA15 and copper sheet is shown in Fig. 3. In the figure, the reaction layer contains three reaction products marked as A-C sorted by their shapes and colors. The dark gray phase A with cellular structure is located next to TA15. Light gray phase B with dendritic structure takes the majority of the reaction products and grew into the copper interlayer. Granular phase C of bright gray color lays in the clearance of the dendrites. Scanning electron microscope-energy dispersive spectrum (SEM-EDS) analysis was applied to phases A-C to measure the compositions of the reaction products as listed in Table 4. Combining with Ti-Cu binary phase diagram (Fig. 4) (Ref 16), we could conclude that phases A-C were CuTi, Cu_4Ti_3, and Cu_2Ti intermetallics. XRD analysis also confirmed the existence of the above phases (Fig. 5).

Now, the detailed process of the contact reaction could be deduced. The existence temperature range of the reaction products acquired from Ti-Cu binary phase diagram is listed in Table 5. It was clear that CuTi with cellular structure grew up in the region next to the titanium alloy where the cooling rate was highest in the weld pool, which indicated that it crystallized first during the cooling stage. Cu_4Ti_3 taking on dendritic structure implied that it also formed in the early stage. While Cu_2Ti with granular structure lying among Cu_4Ti_3 dendrites showed that it appeared finally. In conclusion, the forming sequence of these three compounds was CuTi, Cu_4Ti_3, and Cu_2Ti.

The contact reactive process between copper interlayer and titanium alloy could be divided into two steps as follows:

(1) The process of liquid formation during the heating stage. This process included two proceedings. One was the interdiffusion of Ti and Cu elements until the material with eutectic composition (Ti 73 at.%, Cu 27 at.%) in the interface was achieved. At this moment, the initial liquid emerged by the eutectic reaction at the eutectic temperature. The other was the dissolution of base metal into the initial liquid phase. Because the diffusion ability

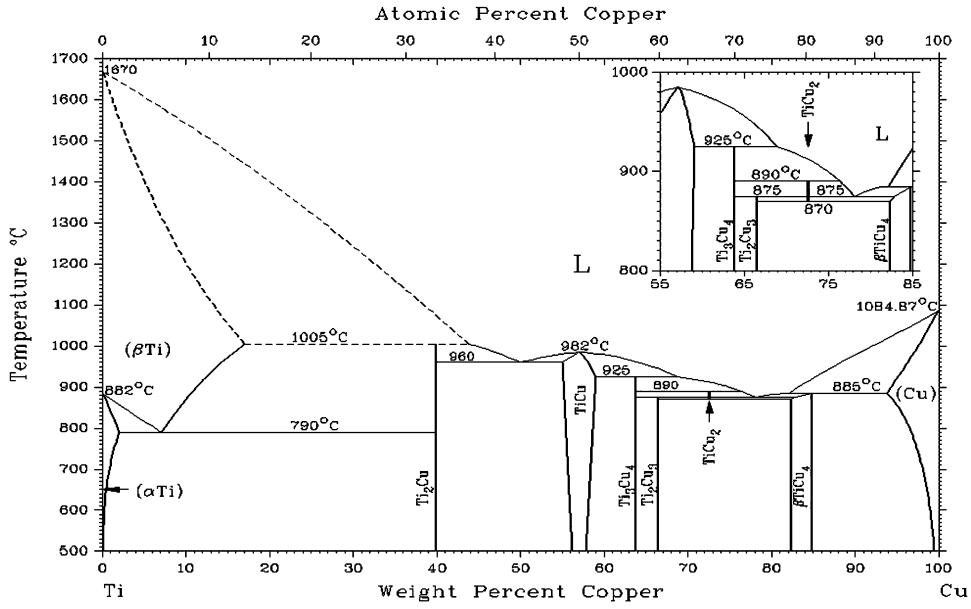

Fig. 4 Ti-Cu binary phase diagram

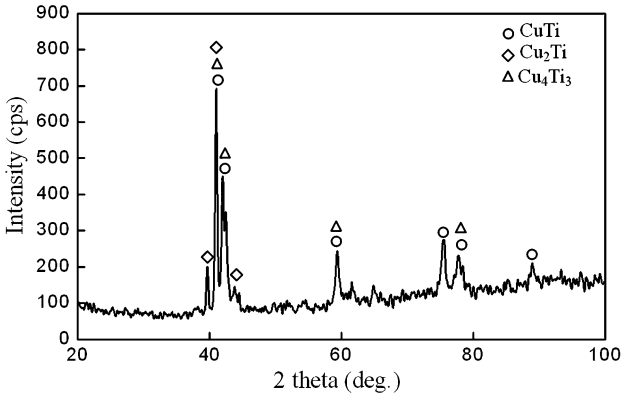

Fig. 5 X-ray diffractogram of reactive layer

Table 5 Existence temperature range of various reaction phases (°C)

CuTi	Cu_4Ti_3	Cu_2Ti
<982	<925	890-870

of Ti into Cu was stronger than that of Cu into Ti (Ref 2), a larger area of copper than TA15 in solid state dissolved into the liquid.

(2) The process of the three reaction products forming during the cooling stage. Firstly, the congruent melting compound TiCu crystallizing next to titanium alloy conformed to the transformation: L → CuTi. Then the content of Cu in the residual liquid increased, which resulted in the peritectic reaction (L + CuTi → Cu_4Ti_3). Cu_4Ti_3 phase grew up along the largest temperature gradient direction in the liquid. The residual liquid was pushed into the clearance of the Cu_4Ti_3 dendrites. Finally, the peritectic reaction (L + Cu_4Ti_3 → Cu_2Ti) occurred and granular Cu_2Ti phase formed. It was needed to notice that Cu_2Ti was a kind of metastable phase existing in the temperature range of 890-870 °C from Table 5. But in this paper it was found at room temperature because the high temperature phase Cu_2Ti was retained for the rapid cooling rate during electron beam welding.

As is well known, the thickness of the intermetallics layer is significantly affected by the heat input. The microstructures of the reactive layers in the joints under different welding parameters were examined in this paper, as given in Fig. 6.

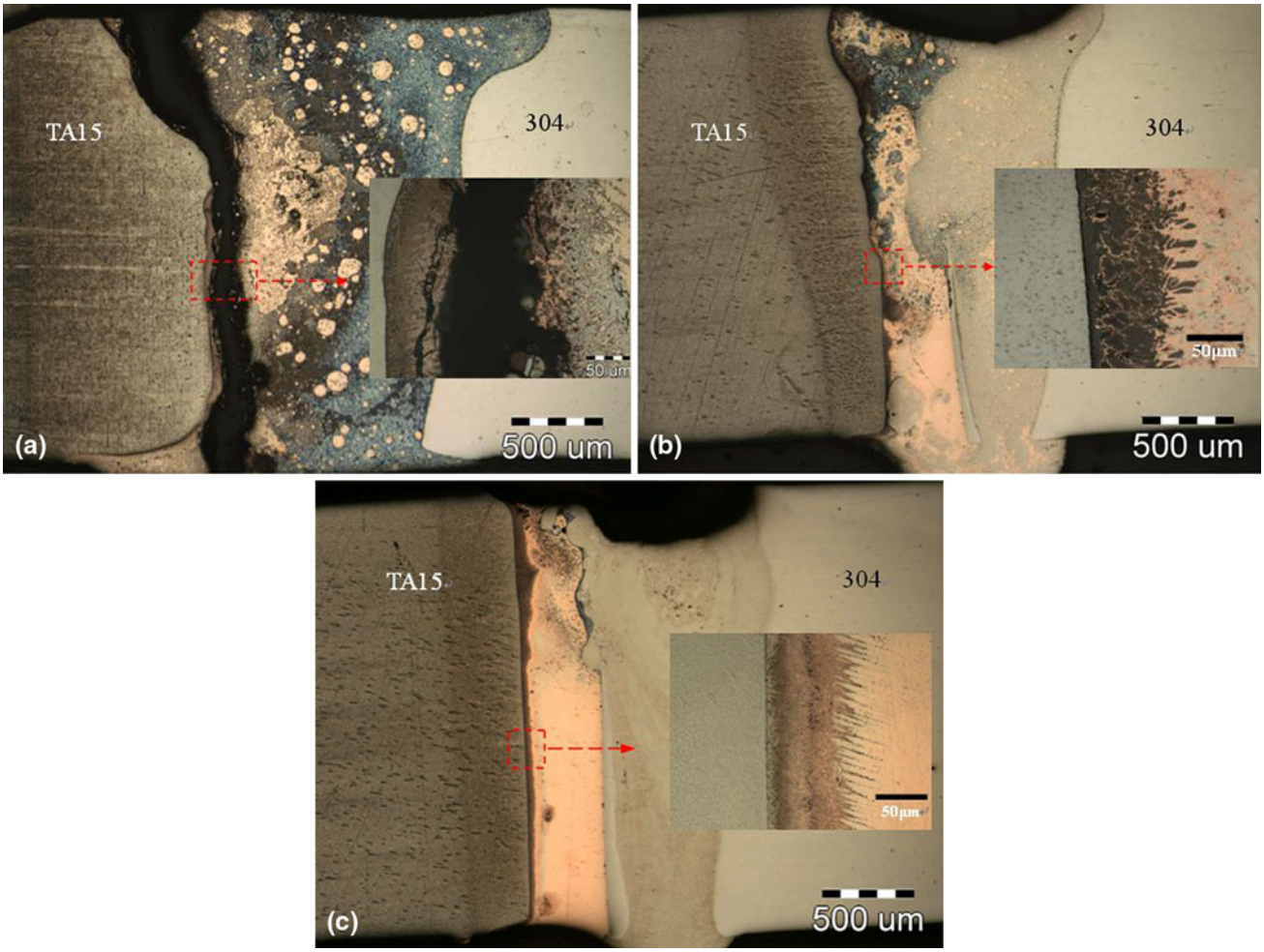

Fig. 6 Microstructures of the reaction layer in the joints under different welding parameters: (a) I_b = 11 mA, v = 5 mm s^{-1}; (b) I_b = 13 mA, v = 8.33 mm s^{-1}; (c) I_b = 11 mA, v = 8.33 mm s^{-1}

It can be seen that almost the whole copper sheet melted when the heat input was the highest, and the joint fractured immediately after welding. With the decrease of the heat input, the more volume of copper sheet remained solid state during welding process. Finally, more soft pure copper was located in the joint, which can relieve the thermal stress in the joint. Comparing Fig. 6(b) and (c), it can be seen that thicknesses of the reactive interlayers in the joints under different beam currents were very similar. This may be due to the high cooling rate in electron beam welding process, the thickness of the intermetallics layer was only dependent on the initial liquid volume, but the beam current mostly affect the diffusion process after the liquid of Ti and Cu solidified.

3.2.2 Fusion Welding of Copper Sheet to 304 at the Top. As above mentioned, at the top of the joint, copper interlayer and 304 stainless steel were joined by fusion welding. The microstructure of the weld zone is given in Fig. 7. From the figure we could see that the weld was mainly made up of solidified stainless steel with a small amount of copper. Due to the extremely low solubility of copper in iron, copper existed in the form of elemental crystal.

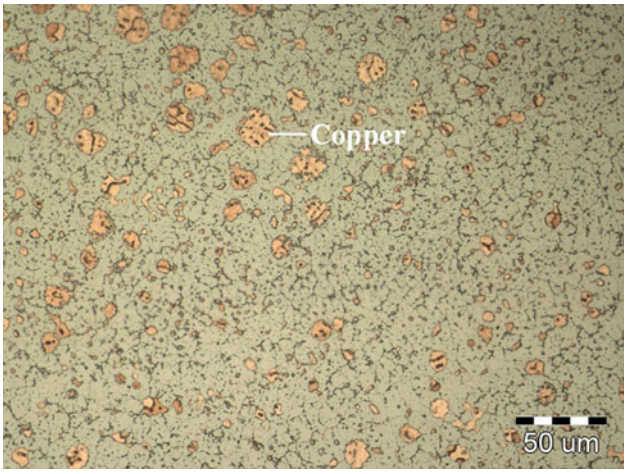

Fig. 7 Microstructure of the weld between copper interlayer and stainless steel

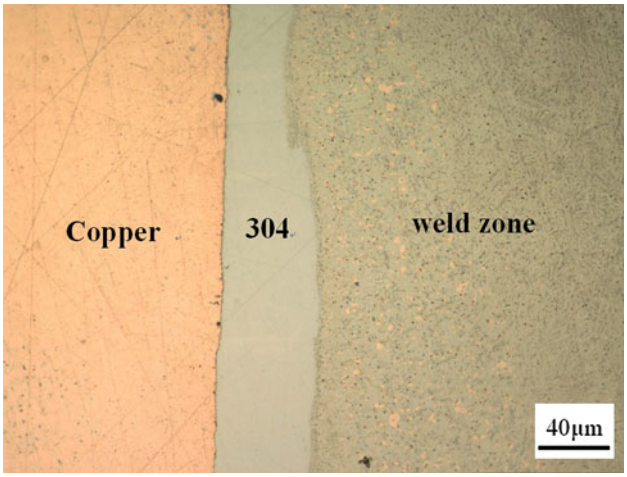

Fig. 8 Interface between copper interlayer and 304 stainless steel at the bottom of the joint

3.2.3 Diffusion Bonding of the Copper Sheet to 304 at the Bottom. The interface between copper interlayer and 304 stainless steel at the bottom of the joint is shown in Fig. 8. It was clear that the profile of the interface remained straight and no defect was found, which indicated that they were well diffusion bonded in a short time. The concentration profiles close to the interface of Fe and Cu measured by EPMA (electron probe microanalysis) was given in Fig. 9(a). From the figure, it was clear that about 0.5 μm thick diffusion layers of Cu in 304 stainless steel and Fe in the copper sheet existed.

In order to confirm the feasibility of the diffusion phenomenon, a simplified computation of the diffusion distance was carried out by one-dimensional steady state Fick's Law in the form of the error function. The concentration of Cu and Fe can be denoted as Eq 1:

$$c = \frac{c_s}{2}\mathrm{erfc}\left(\frac{x}{2\sqrt{Dt}}\right) \quad \text{(Eq 1)}$$

Here c_s is the initial concentration, x is the diffusion distance, t is the diffusion time, and D is the diffusion coefficient.

Solve this function with the initial condition (when $t = 0$) that $c = c_s$ when $x < 0$ and $c = 0$ when $x < 0$. The diffusion coefficients D_{Fe} and D_{Cu} were 3.87×10^{-11} and 5.68×10^{-11} cm^2 s^{-1} reported by Yilmaz et al. (Ref 17). In fact, diffusion coefficients are temperature dependent, but in this

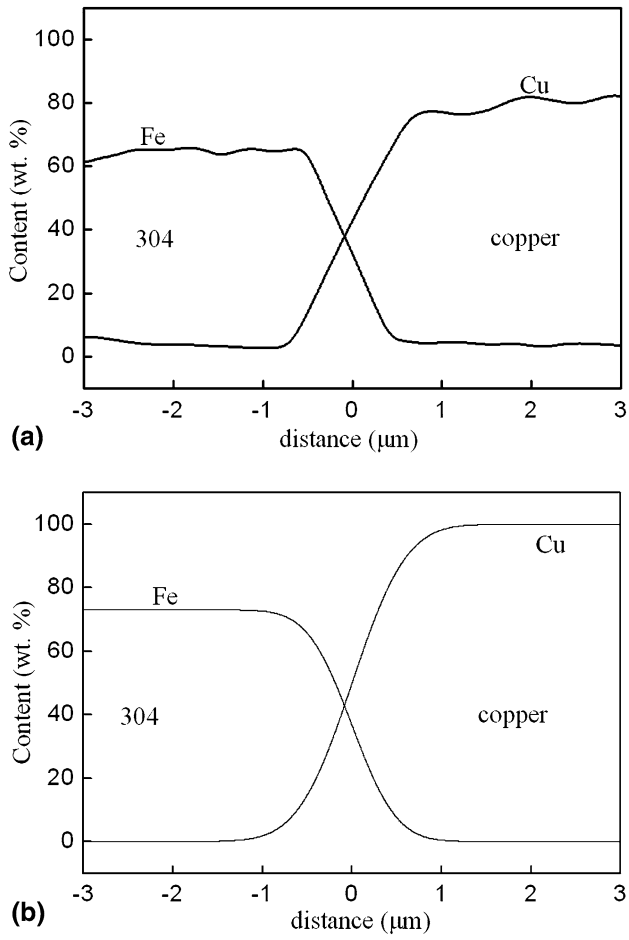

Fig. 9 Concentration profiles of Cu and Fe close to the interface: (a) measured by EPMA, (b) computed

paper we treated as a constant value for the temperature in the weld is difficult to measure. And here we just want to theoretically verify whether the diffusion process can implement or not, but not to give an exact solution. The computed concentration profiles of Cu and Fe (let $t = 20$ s) are given in Fig. 9(b). It was proved that a diffusion layer with the thickness of approximately 0.5 μm could form in about 10-20 s and it can be satisfied by using the welding parameters described in Sect. 2. Diffusion pressure was supplied by the compressive load and the thermal stress.

3.3 Mechanical Properties

The tensile strengths of the joints under different beam currents were listed in Table 6. The tensile strength can reach to 300 MPa, up to 55% of that of 304 stainless steel, which was higher than that of most diffusion bonding joints between titanium alloy and stainless steel (Ref 7, 18-21). To find the weakest part of the joint, the fracture location was analyzed as shown in Fig. 10. It was clear that fracture occurred in the interfacial intermetallic compound layer, perpendicular to the tension orientation. The microhardness of CuTi and Cu_4Ti_3 was measured by UMH tester and it was listed in Table 7. The hardness values of the two compounds were much lower than that of Ti-Fe intermetallics (above 1000 HV), which help to gain joints with higher bonding strength.

In addition, we can see that the tensile strength of the joint welded at beam current of 11 mA is higher than that of the joint welded at 13 mA. It may be attributed to the different volumes of the unmelted copper sheets in the two joints since the thickness of the Ti-Cu intermetallic layers are similar. The soft copper is helpful to relieve and accommodate the thermal stress in the dissimilar metals joint. As a result, the ultimate tensile strength of the joint containing a larger amount of the unmelted copper interlayer is higher.

Table 6 Tensile strengths of the joints welded under different beam currents

Joints	Tensile strength (MPa)	Strength factor (with regard to 304 stainless steel)
304SS	550	1.0
TA15	920	…
I_b = 13 mA, v = 8.33 mm s^{-1}	260	0.47
I_b = 11 mA, v = 8.33 mm s^{-1}	300	0.55

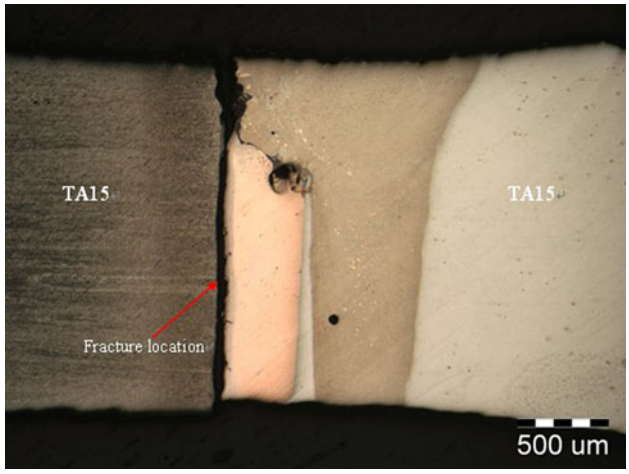

Fig. 10 Microstructure near the fracture location of the joint

Table 7 Microhardness of various phases (HV)

CuTi	Cu_4Ti_3
560 ± 25	530 ± 25

4. Conclusion

Titanium alloy and stainless steel were well joined heated by electron beam via adding a copper interlayer. The joint was a combination of three kinds of metallurgical process including contact reaction between titanium and copper, fusion welding, and solid state diffusion bonding between copper and stainless steel. The tensile strength can reach to 300 MPa, up to 55% of that of 304 stainless steel. The contact reactive layer mainly contained CuTi, Cu_4Ti_3, and Cu_2Ti intermetallics, and its thickness is hardly due to the heat input for the rapid cooling rate during electron beam welding. The tensile strength is mostly dependent on the volume of the unmelted copper sheet, although the intermetallics layer was the weakest part of the joint and fracture occurred in it during the tensile tests.

Acknowledgments

This work was supported by the National Natural Science Fund, CASC-HIT United Innovation Project, and the National Basic Research Program of China.

References

1. R.R. Boyer, An Overview on the Use of Titanium in the Aerospace Industry, *Mater. Sci. Eng. A*, 1996, **213**, p 103–114
2. J.L. Yang, Y. Li, and F. Wang, New Application of Stainless Steel, *J. Iron Steel Res. Int.*, 2006, **13**(1), p 62–66
3. A. Fuji, K. Ameyama, and T.H. North, Improved Mechanical Properties in Dissimilar Ti-AISI, 304L Joints, *J. Mater. Sci.*, 1996, **31**, p 819–827
4. B. Qin, G.M. Sheng, and J.W. Huang, Phase Transformation Diffusion Bonding of Titanium Alloy with Stainless Steel, *Mater. Charact.*, 2006, **56**, p 32–38
5. N. Orhan, T.I. Khan, and M. Eroglu, Diffusion Bonding of a Microduplex Stainless Steel to Ti-6Al-4V, *Scripta Mater.*, 2001, **45**, p 441–446
6. B. Aleman, I. Gutierrez, and J.J. Urcola, Interface Microstructure in Diffusion Bonding of Titanium Alloys to Stainless and Low Alloy Steels, *Mater. Sci. Technol.*, 1993, **9**, p 633–641
7. S. Kundu and S. Chatterjee, Characterization of Diffusion Bonded Joint Between Titanium and 304 Stainless Steel Using a Ni Interlayer, *Mater. Charact.*, 2008, **59**(5), p 631–637
8. E. Atasoy and N. Kahraman, Diffusion Bonding of Commercially Pure Titanium to Low Carbon Steel Using a Silver Interlayer, *Mater. Charact.*, 2008, **59**, p 1481–1490
9. S. Kundu and S. Chatterjee, Interface Microstructure and Strength Properties of Diffusion Bonded Joints of Titanium-Al Interlayer-18Cr-8Ni Stainless Steel, *Mater. Sci. Eng. A*, 2010, **527**, p 2714–2719

10. S. Kundu and M. Ghosh, Diffusion Bonding of Commercially Pure Titanium to 304 Stainless Steel Using Copper Interlayer, *Mater. Sci. Technol.*, 2005, **13**, p 154–160
11. H. Nishi, Notch Toughness Evaluation of Diffusion-Bonded Joint of Alumina Dispersion—Strengthened Copper to Stainless Steel, *Fusion Eng. Des.*, 2006, **81**, p 269–274
12. I. Magnabosco, P. Ferro, and F. Bonollo, An Investigation of Fusion Zone Microstructures in Electron Beam Welding of Copper-Stainless Steel, *Mater. Sci. Eng. A*, 2006, **424**, p 163–173
13. M.F. Wu, C. Yu, Z.S. Yu, and R.F. Li, Formation Process of Liquid in Interface of Ti/Cu Contact Reaction Couple, *Trans. Nonferrous Met. Soc. China*, 2005, **15**(1), p 125–129
14. T.D. Uzunov, S.P. Stojanov, and S.I. Lambov, Contact-Reactive Welding of Titanium Via Copper Layer, *Vacuum*, 1999, **52**, p 365–368
15. ASTM E8M-04, "Standard Test Methods for Tension Testing of Metallic Materials"
16. J.L. Murray, The Cu-Ti (Copper-Titanium) System, *J. Phase Equilib.*, 1983, **4**(1), p 81–95
17. O. Yilmaz and M. Aksoy, Investigation of Micro-crack Occurrence Conditions in Diffusion Bonded Cu-304 Stainless Steel Couple, *J. Mater. Process. Technol.*, 2002, **121**, p 136–142
18. M. Ghosh and S. Chatterjee, Diffusion Bonded Transition Joints of Titanium to Stainless Steel with Improved Properties, *Mater. Sci. Eng. A*, 2003, **358**, p 152–158
19. M. Ghosh and S. Chatterjee, Effect of Interface Microstructure on the Bond Strength of the Diffusion Welded Joints Between Titanium and Stainless Steel, *Mater. Charact.*, 2005, **54**, p 327–337
20. P. He, X. Yue, and J.H. Zhang, Hot Pressing Diffusion Bonding of a Titanium Alloy to a Stainless Steel with an Aluminum Alloy Interlayer, *Mater. Sci. Eng. A*, 2008, **486**, p 171–176
21. S. Kundu and S. Chatterjee, Interface Microstructure and Strength Properties of Diffusion Bonded Joints of Titanium-Al Interlayer—18-8Cr-8Ni Stainless Steel, *Mater. Sci. Eng. A*, 2010, **527**, p 2714–2719